Phonon-scattering-limited electron mobilities in $Al_xGa_{1-x}As/GaAs$ heterojunctions

T. Kawamura and S. Das Sarma
Joint Program for Advanced Electronic Materials, Department of Physics, University of Maryland, College Park, Maryland 20742-4111
(Received 10 June 1991)

We study the bulk-phonon-scattering contribution to the transport properties of a two-dimensional electron gas formed at the interface of an ultrapure $Al_xGa_{1-x}As/GaAs$ heterojunction. Assuming that the electrons only occupy the lowest subband, we calculate the mobility as a function of temperature for the temperature range $T=1-300$ K, within the variational-subband-wave-function model for carrier confinement. Our work encompasses three physically distinct temperature ranges with respect to phonon scattering: the Block-Grüneisen (BG), equipartition (EP), and inelastic regimes. In the EP regime we calculate (i) the individual and total scattering rates τ_s^{-1}, and momentum relaxation rates τ_t^{-1}, due to deformation-potential and piezoelectric coupled acoustic-mode phonons, with screening of these rates taken into account within the static random-phase approximation; (ii) the acoustic-phonon-scattering limited drift mobilities μ_{ac} for different densities n_s as a function of temperature T; (iii) the level of validity of Matthiessen's rule; and (iv) the dimensionless Hall ratio r_H. In addition, we investigate in detail the temperature dependence of the low-temperature mobility and find excellent agreement with experimental data for the linear coefficient $\alpha=d\mu^{-1}(T)/dT$ of the temperature dependence as a function of density. We carry out similar calculations in the BG regime and compare the results with the corresponding ones in the EP regime. Finally, to evaluate the mobility in the inelastic regime at high temperatures above $T\approx 40$ K, where the scattering from polar LO phonons becomes important, we compute the first-order perturbation distribution $\phi(E)$ as a function of the carrier energy E by directly solving the linearized Boltzmann equation by an iterative method. We compare these results with the commonly used closed-form approximations for ϕ: the low-temperature relaxation-time approximation τ_{LT}, and the high-energy relaxation-time approximation τ_{HE}, and check their level of validity.

I. INTRODUCTION

A great deal of experimental and theoretical effort has been focused on the transport properties of a two-dimensional electron gas (2DEG) in high-mobility, modulation-doped $Al_xGa_{1-x}As/GaAs$ heterojunctions. The fabrication of extremely pure samples with electron mobilities higher than 10^6 cm^2/V s is now commonplace, and mobilities in excess of 10^7 cm^2/V s have also been achieved at low temperatures.[1,2] Scattering mechanisms which are responsible for limiting the mobility in heterolayers can be categorized as being either of the extrinsic or intrinsic type. Extrinsic effects associated with charged impurity scattering due to unintentional doping of the bulk GaAs and the $Al_xGa_{1-x}As$ spacer layer can in principle be reduced by improving growth and fabrication techniques. This is not the case for scattering from the remote ionized impurities in the highly doped $Al_xGa_{1-x}As$ region, which is considered to be an intrinsic effect, since they are responsible for contributing the electronic space charge which constitutes the 2DEG at the heterointerface. In addition, at any finite temperature the electrons are unavoidably subjected to the intrinsic scattering effects due to the absorption and emission of phonons. It follows that the inherent limit of the highest achievable mobility in such structures is determined by the scattering from the remote ions, and the relevant phonons. In principle, at least, it is the phonon scattering which sets the ultimate limit on the highest achievable theoretical mobility at any particular temperature.

In this paper we focus on a thorough understanding of the transport properties, as determined by the bulk phonon contribution to the intrinsic scattering by phonons in a GaAs-based 2DEG in the temperature range $T=1-300$ K. With respect to phonon scattering, our study encompasses three physically distinguishable temperature ranges: (i) the Bloch-Grüneisen (BG), (ii) equipartition (EP), and (iii) inelastic regimes.

At low temperatures below $T\approx 40$ K the electrons in the GaAs channel are scattered via deformation-potential (DP) and piezoelectric- (PE) coupled acoustic-mode phonons. For typical carrier densities $n_s\approx 10^{11}$ cm^{-2}, the thermal energy k_BT (where k_B is Boltzmann's constant) is much smaller than the Fermi energy of the 2DEG. In the EP regime, which begins approximately above $T\approx 4$ K, the available acoustic-phonon energies are much smaller than k_BT so that the scattering is quasielastic, and the equilibrium Bose occupation factor can accurately be replaced by a linear term in T. The evaluation of the relevant scattering rates is greatly facilitated in the EP regime since the absorption and emission rates become equivalent, and quasielasticity allows us to rigorously define a closed-form expression for the momentum relaxation time. Most of the current work in the field has been heavily focused in the EP regime from

$T \approx 4$ to 40 K, where the reciprocal mobility μ^{-1} exhibits a simple linear dependence on temperature. The slope of the curve determines the linear coefficient of the temperature dependence of the low-temperature mobility $\alpha = d\mu^{-1}/dT$, which contains important information about the electron-phonon interactions operative in heterojunctions. For temperatures below $T \approx 4$ K, in the BG regime where the acoustic phonon and thermal energies are comparable, it is expected that the transport properties will be dominated by the remote ions. As a result, not as much detailed study has been focused on phonon scattering at extremely low temperatures. In the BG regime the constraints of degeneracy and energy conservation lead to a drastic reduction in the momentum relaxation rate at the Fermi energy, due to phase-space restriction for scattering via acoustic phonons. This results in a much stronger dependence of the reciprocal mobility on temperature. For high temperatures above $T \approx 40$ K, the inelastic scattering from the polar LO phonons begin to play an increasingly important role in determining the transport properties. This scattering mechanism is inelastic and nonrandomizing so that it is no longer possible to strictly define a universal momentum relaxation time. In this case one must directly solve the appropriate linearized Boltzmann equation.

In the EP regime we calculate (i) the individual and total scattering rates τ_s^{-1}, and momentum relaxation rates τ_t^{-1}, due to DP and PE-coupled acoustic-mode phonons, with screening of these rates taken into account within the static random-phase approximation (RPA); (ii) the acoustic-phonon-scattering limited drift mobilities μ_{ac} for different densities n_s as a function of temperature T; (iii) the level of validity of Matthiessen's rule; and (iv) the dimensionless Hall ratio r_H. In addition we investigate in detail the temperature dependence of the low-temperature mobility and find excellent agreement with experimental data for the linear coefficient $\alpha = d\mu^{-1}(T)/dT$ of the temperature dependence as a function of density. We carry out similar calculations in the BG regime and compare the results with the corresponding ones in the EP regime. Finally, to evaluate the mobility in the inelastic regime at high temperatures above $T \approx 40$ K, where the scattering from polar LO phonons starts to become important, we compute the first-order perturbation distribution $\phi(E)$ as function of the carrier energy E by directly solving the linearized Boltzmann equation by an iterative method. We compare these results with the commonly used closed-form approximations for ϕ—the low-temperature relaxation-time approximation τ_{LT} and the high-energy relaxation time approximation τ_{HE}—and check their level of validity. In all three regime we use the same theoretical model based on the variational-subband wave function where we assume that all the electrons occupy the lowest subband, and that the important scattering is via bulk phonons.

II. BASIC TRANSPORT THEORY

The transport coefficients of a two-dimensional electron gas (2DEG) have been investigated by a number of workers. In this section we review briefly the theoretical model adopted in our calculation of the bulk-phonon-scattering limited mobilities in the three temperature ranges discussed earlier.

A. Boltzmann equation

Let $f(\mathbf{r},\mathbf{k},t)$ denote the distribution function which gives the occupation probability of the state $|\mathbf{k}\rangle$ by an electron in a volume element $d\mathbf{r}$ at position $\mathbf{r}$ at time t. The rate of change of $f(\mathbf{r},\mathbf{k},t)$ with respect to time is given for the familiar Boltzmann equation

$$\frac{\partial f}{\partial t} = -\frac{1}{\hbar}\frac{\partial E}{\partial \mathbf{k}}\cdot\frac{\partial f}{\partial \mathbf{r}} - \frac{1}{\hbar}\mathbf{F}\cdot\frac{\partial f}{\partial \mathbf{k}} + I_c[f] , \tag{1}$$

where E is the electron energy, $\mathbf{F}$ is the force due to the externally applied electric field, and $\hbar$ is the reduced Planck constant. The last term is the collision integral, which arises from electron scattering and is given by

$$I_c[f] = -\int \frac{d^3k'}{(2\pi)^3}\{S(\mathbf{k},\mathbf{k}')f(\mathbf{r},\mathbf{k},t)[1-f(\mathbf{r},\mathbf{k}',t)] - S(\mathbf{k}',\mathbf{k})f(\mathbf{r},\mathbf{k}',t) \times [1-f(\mathbf{r},\mathbf{k},t)]\} , \tag{2}$$

where $S(\mathbf{k},\mathbf{k}')$ is the differential scattering rate from state $|\mathbf{k}\rangle$ to state $|\mathbf{k}'\rangle$. For a uniform electric field in a homogeneous system, the Boltzmann equation in the steady state becomes

$$\frac{1}{\hbar}\mathbf{F}\cdot\frac{\partial f(\mathbf{k})}{\partial \mathbf{k}} = I_c[f] . \tag{3}$$

In equilibrium the carrier distribution is simply given by the Fermi-Dirac occupation factor,

$$f_0(E) = \frac{1}{\exp[\beta(E-\zeta)]-1} , \tag{4}$$

where ζ is the chemical potential and $\beta = 1/k_B T$. In the presence of an electric field, the distribution function f experiences an axially symmetric perturbation which is biased towards the field direction. In this case f may be expanded in terms of Legendre polynomials[3] $P_n(\cos\alpha)$, where α is the angle between $\mathbf{k}$ and $\mathbf{F}$:

$$f(\mathbf{k}) = \sum_n f_n(E)P_n(\cos\alpha) . \tag{5}$$

For low electric fields we need only keep the first two terms of the series so that

$$f(\mathbf{k}) = f_0 - \frac{e\hbar F}{m^*}k\cos\alpha\frac{\partial f_0}{\partial E}\phi(E) , \tag{6}$$

where we have taken $f_1(E) = -(e\hbar/m^*)k(\partial f_0/\partial E)\phi(E)$ to simplify the algebra.[4,3] The isotropic effective mass of the carriers is denoted by m^*, the electronic charge by e, and $\phi(E)$ is the perturbation distribution which has units of s^{-1}. Using the principle of detailed balance,

$$S(\mathbf{k},\mathbf{k}')f_0(E)[1-f_0(E')] = S(\mathbf{k}',\mathbf{k})f_0(E')[1-f_0(E)] , \tag{7}$$

we can derive a simplified form for the collision integral,[4,3]

$$I_c[f]=-\frac{e\hbar F}{m^* k_B T}k\cos\alpha \times\int\frac{d^3k'}{(2\pi)^3}f_0(E)[1-f_0(E')] \times\left[\phi(E)-\frac{k'\cos\theta}{k}\phi(E')\right]S(\mathbf{k},\mathbf{k}') , \quad (8)$$

where θ is the angle between $\mathbf{k}$ and $\mathbf{k}'$. Substituting Eq. (8) into Eq. (3) we arrive at the linearized Boltzmann equation,[4,3]

$$1=\int\frac{d^3k'}{(2\pi)^3}\frac{[1-f_0(E')]}{[1-f_0(E)]} \times\left[\phi(E)-\frac{k'\cos\theta}{k}\phi(E')\right]S(\mathbf{k},\mathbf{k}') . \quad (9)$$

B. Scattering theory in a 2DEG

The carriers in an $Al_xGa_{1-x}As/GaAs$ heterojunction are spatially confined along the normal direction with respect to the interface, which we designate as the z direction. As a result of the intrinsic internal field in the heterojunction, there is no longer any translational invariance along z, so that the wave function of an electron is given by

$$\Psi_n(\mathbf{r},z)=\xi_n(z)\exp(i\mathbf{k}\cdot\mathbf{r}) , \quad (10)$$

where $\xi_n(z)$ is the electric subband wave function, $\mathbf{k}$ is the 2D electron wave vector in the plane, and $\mathbf{r}\equiv(x,y)$. In this section we denote all 3D vectors and their magnitudes by capital letters, distinguishing them from the strictly 2D ones. The corresponding energy of the state Ψ_n is given by

$$E_n(\mathbf{k})=E_n+\frac{\hbar^2k^2}{2m^*} , \quad (11)$$

where we have assumed a parabolic energy band, and $m^*=0.067m_0$ is the effective mass in GaAs. In what follows we assume that the electrons only occupy the lowest subband ($n=0$), and that the confinement profile is accurately described by the variational wave function

$$\xi_0(z)=\sqrt{\tfrac{1}{2}b^3z^2}\exp(-\tfrac{1}{2}bz) , \quad (12)$$

where b is a variational parameter given by

$$b=\left[\frac{48\pi m^* e^2}{\epsilon_0\hbar^2}\right]^{1/3}(n_{\rm depl}+\tfrac{11}{32}n_s)^{1/3} . \quad (13)$$

Here, $\epsilon_0=12.91$ is the static dielectric constant in GaAs, n_s is the 2D sheet density, and $n_{\rm depl}$ is the depletion charge per unit area in the channel.

C. Acoustic-phonon scattering

In this paper we consider the scattering of electrons arising from the absorption and emission of acoustic-mode phonons and polar LO phonons. Consistent with all previous work in the field, we assume that the phonon modes in a heterojunction remain unaltered from those in bulk GaAs. Although it may be an oversimplification of the actual situation, we consider the interface phonons to contribute insignificantly to the scattering of the electrons. Taking $\mathbf{k}$ and $\mathbf{k}'$ to denote the 2D electron wave vectors before and after scattering, respectively, by a bulk phonon with 3D wave vector $\mathbf{Q}$, with components $(\mathbf{q},q_z)$ within and normal to the heterolayer, momentum conservation in the x-y plane gives us that $q=|\mathbf{k}-\mathbf{k}'|$. In the z direction, in place of momentum conservation we must carry out an integration over the perpendicular component of the phonon wave vector q_z. In particular, the differential scattering rate between 2D electrons $S_{\rm II}$ is simply calculated from the 3D transition rate $S_{\rm III}$ from the relation[5–8]

$$S_{\rm II}=\int|I(q_z)|^2S_{\rm III}dq_z , \quad (14)$$

where $I(q_z)$ is the overlap for intraband scattering,

$$I(q_z)=\int\xi_0^2(z)\exp(iq_zz)dz . \quad (15)$$

Substituting Eq. (12) into Eq. (15), we obtain

$$|I(q_z)|^2=\frac{b^6}{(b^2+q_z^2)^2} . \quad (16)$$

It follows that as long as the 3D rates $S_{\rm III}$ are known, it is a straightforward task to evaluate the corresponding 2D rates $S_{\rm II}$.

The 3D differential scattering rate can be written in the form[6]

$$S_{\rm III}=\frac{2\pi}{\hbar}|C_j(Q)|^2\Delta(E,E') , \quad (17)$$

where the matrix elements $|C_j(Q)|^2$ for DP, longitudinal PE, and transverse PE-coupled scattering are given by[6]

$$|C_{\rm DP}(Q)|^2=\frac{D^2\hbar Q}{2\rho u_l} , \quad (18a)$$

$$|C_{{\rm PE};l}(Q)|^2=\frac{(eh_{14})^2\hbar u_l}{2\rho u_l}\frac{1}{Q}A_l(Q) , \quad (18b)$$

$$|C_{{\rm PE};t}(Q)|^2=\frac{(eh_{14})^2\hbar u_t}{2\rho u_t}\frac{1}{Q}A_t(Q) . \quad (18c)$$

We consider the inelastic scattering from LO phonons in a following section. Here, D is the DP constant, $h_{14}=1.2\times10^7$ V/cm is the applicable PE tensor component, ρ is the mass density, and u_l (u_t) is the longitudinal (transverse) velocity of sound in GaAs. The functions $A_{l,t}(Q)$ are the dimensionless anisotropy factors for a (001) heterolayer orientation in a crystal with zinc-blende symmetry.[6] Expressed in terms of the bulk 3D phonon wave-vector components $\mathbf{Q}\equiv(\mathbf{q},q_z)$, they are given by

$$A_l(q,q_z)=\frac{9q_z^2q^4}{2(q_z^2+q^2)^3} , \quad (19a)$$

$$A_l(q,q_z)=\frac{8q_z^4q^2+q^6}{4(q_z^2+q^2)^3} \ . \tag{19b}$$

The factor $\Delta(E,E')$ is given by

$$\Delta(E,E')=N_Q\delta(E-E'+\hbar\omega_Q) +(N_Q+1)\delta(E-E'-\hbar\omega_Q)\Theta(E-\hbar\omega_Q) \ , \tag{20}$$

where $\Theta(x)$ is the unit-step function. The first (second) term corresponds to the absorption (emission) of an acoustic phonon of wave vector $\mathbf{Q}$, and energy $\hbar\omega_Q=\hbar u_{l,t}(q^2+q_z^2)^{1/2}$. For low fields the phonon distribution $N(Q)$ is in equilibrium and is given by the usual Bose occupation factor

$$N_Q=\frac{1}{\exp(\beta\hbar\omega_Q)-1} \ . \tag{21}$$

The 2D version of the linearized Boltzmann equation Eq. (9) is given by

$$1=\frac{1}{(2\pi)^3}\frac{2\pi}{\hbar}\int d^2k'\int dq_z\frac{[1-f_0(E')]}{[1-f_0(E)]} \times\left[\phi(E)-\frac{k'\cos\theta}{k}\phi(E')\right] \times|I(q_z)|^2\frac{|C_j(q,q_z)|^2}{\epsilon^2(q,T)}\Delta(E,E') \ , \tag{22}$$

where j denotes the different acoustic-phonon-scattering mechanisms under consideration. This equation forms the basis of our analysis of the transport properties of a 2DEG. Note that we have introduced the effects of screening[9] on the bare scattering rates by dividing the matrix elements $C_j(q,q_z)$ by the dielectric function $\epsilon(q,T)$, of the 2DEG,

$$\epsilon(q,T)=1+\frac{2\pi e^2}{\epsilon_0 q}H(q)\Pi(q,T) \ . \tag{23}$$

We use the Maldague formula to calculate the static finite temperature polarizability,[10,11]

$$\Pi(q,T,\zeta)=\int_0^\infty\frac{\Pi_0(q,\zeta')}{4k_BT\cosh^2[(\zeta-\zeta')/2k_BT]}d\zeta' \ . \tag{24}$$

Here, Π_0 is the zero-temperature RPA polarizability function of the 2DEG

$$\Pi_0(q)=\frac{m^*}{\pi\hbar^2}\left\{1-\Theta(q-2k_F)\left[1-\left[\frac{2k_F}{q}\right]^2\right]\right\} \ , \tag{25}$$

where k_F denotes the Fermi wave vector. The form factor $H(q)$ associated with the subband wave function is defined by

$$H(q)=\int dz\int dz'\xi_0^2(z)\xi_0^2(z')\exp(-q|z-z'|) \ . \tag{26}$$

Substituting Eq. (13) into Eq. (27) we obtain[5]

$$H(q)=\frac{8+9w+3w^2}{8(1+w)^3} \ , \tag{27}$$

where $w=q/b$.

The scattering of electrons from acoustic phonons may be considered quasielastic since $\hbar\omega_Q\ll E_F$, where E_F is the Fermi energy. In the EP temperature range we have that $\hbar\omega_Q/k_BT\ll1$ so that $N_Q\sim k_BT/\hbar\omega_Q$. Under these approximations Eq. (22) takes the simplified form

$$\phi^{-1}(E)=\frac{1}{(2\pi)^3}\frac{2\pi}{\hbar} \times\int d^2k'\int dq_z(1-\cos\theta) \times|I(q_z)|^2\frac{|C_j(q,q_z)|^2}{\epsilon^2(q,T)}\Delta(E,E') \ , \tag{28}$$

where $\Delta(E,E')=(2k_BT/\hbar\omega_Q)\delta(E-E')$ and $q^2=2k^2(1-\cos\theta)$. From Eq. (28) we see that for quasielastic scattering the perturbation distribution $\phi(E)$ is easily calculated in a closed form. The solution obtained in this way is called the relaxation time $\tau_t(E)$, since from Eq. (6) we see that the collision integral can be written in the form

$$I_c[f]=-\frac{f-f_0}{\tau_t(E)} \ , \tag{29}$$

where $\tau_t(E)=\phi(E)$ is the characteristic time in which the distribution f returns to its equilibrium form f_0 in the absence of the external field F.

Substituting Eqs. (16), (18), and (19) into Eq. (28), we obtain the following expressions for the relaxation time:

$$\frac{1}{\tau_{\rm DP}(E)}=\frac{3D^2m^*bk_BT}{16\pi\hbar^3\rho u_l^2}\int_0^\pi\frac{1}{\epsilon^2(q,T)}(1-\cos\theta)d\theta \ , \tag{30a}$$

$$\frac{1}{\tau_{{\rm PE};l}(E)}=\frac{9}{32}\frac{(eh_{14})^2m^*k_BT}{2\pi\hbar^3\rho u_l^2} \times\int_0^\pi\frac{1}{q\epsilon^2(q,T)}(1-\cos\theta)f_l(w)d\theta \ , \tag{30b}$$

$$\frac{1}{\tau_{{\rm PE};t}(E)}=\frac{13}{32}\frac{(eh_{14})^2m^*k_BT}{2\pi\hbar^3\rho u_t^2} \times\int_0^\pi\frac{1}{q\epsilon^2(q,T)}(1-\cos\theta)f_t(w)d\theta \ , \tag{30c}$$

where f_l (f_t) are the dimensionless form factors for the longitudinal (transverse) acoustic-phonon modes associated with the piezoelectric coupling defined by

$$f_l(w)=\frac{9}{32}\frac{q}{\pi}\int dz\int dz'\int\xi_0^2(z)\xi_0^2(z') \times\int_{-\infty}^{+\infty}\frac{A_l(q,q_z)}{q^2+q_z^2} \times\exp[iq_z(z-z')]dq_z \ , \tag{31a}$$

$$f_t(w)=\frac{13}{64}\frac{q}{\pi}\int dz\int dz'\int \xi_0^2(z)\xi_0^2(z') \times\int_{-\infty}^{+\infty}\frac{A_t(q,q_z)}{q^2+q_z^2} \times\exp[iq_z(z-z')]dq_z \ . \tag{31b}$$

After a contour integration we have

$$f_l(w)=(\tfrac{1}{3})\int dz\int dz'\xi_0^2(z)\xi_0^2(z') \times(3+3u-u^3)\exp(-u) \ , \tag{32a}$$

$$f_t(w)=(\tfrac{1}{13})\int dz\int dz'\xi_0^2(z)\xi_0^2(z') \times(13+13u-14u^2+3u^3)\exp(-u) \ , \tag{32b}$$

where $u=q|z-z'|$. Substituting for the wave function $\xi_0(z)$ we obtain[5]

$$f_l(w)=\frac{1+6w+13w^2+2w^3}{(1+w)^6} \ , \tag{33a}$$

$$f_t(w)=\frac{13+78w+72w^2+82w^3+36w^4+6w^5}{13(1+w)^6} \ . \tag{33b}$$

It is the relaxation time $\tau_j(E)$ which is of relevance to the transport properties, such as the mobility in a 2DEG. As a result of the external dc electric field the distribution function is deformed from f_0, inducing a current density $\mathbf{j}$ given by

$$\mathbf{j}=\frac{1}{2\pi^2}\frac{e}{\hbar}\int\frac{\partial E}{\partial\mathbf{k}}f(\mathbf{k})d^2k \tag{34}$$

in a heterolayer. From the definition of the drift mobility $\mu_D=j/n_sF$, we obtain

$$\mu_D=\frac{e}{m^*}\langle\tau_{\rm tot}(E)\rangle \ , \tag{35}$$

where

$$\langle\tau(E)\rangle=\frac{\int\tau(E)E\left[\frac{\partial f_0}{\partial E}\right]dE}{\int E\left[\frac{\partial f_0}{\partial E}\right]dE} \ . \tag{36}$$

For the Hall mobility μ_H we have that[7]

$$\langle\tau(E)\rangle_{\rm Hall}=\frac{\int\tau^2(E)E\left[\frac{\partial f_0}{\partial E}\right]dE}{\int\tau(E)E\left[\frac{\partial f_0}{\partial E}\right]dE} \ . \tag{37}$$

To calculate the mobility limited by acoustic phonons in a 2DEG we simply take

$$\frac{1}{\tau_{\rm tot}(E)}=\frac{1}{\tau_{\rm DP}(E)}+\frac{1}{\tau_{{\rm PE};l}(E)}+\frac{2}{\tau_{{\rm PE};t}(E)} \ , \tag{38}$$

where in the last term the degeneracy of the transverse modes has been taken into account.

At this point it is important to make a clear distinction between the relaxation time τ_t, which is of direct relevance in evaluating the transport properties from the scattering time τ_s. These two characteristic times of the system under consideration differ by the important $(1-\cos\theta)$ factor. The scattering rate τ_s^{-1} is given by making the replacement $(1-\cos\theta)\rightarrow 1$ in the integrand for the formula for τ_j^{-1} given in Eqs. (30a)–(30c). Physically, the scattering time τ_s simply gives the time between scattering events between an electron and an acoustic phonon. From a many-body-theory viewpoint τ_s is simply related to the imaginary part of the single-particle self-energy due to acoustic-phonon scattering, whereas the relaxation time τ_t is given by a two-particle current-current correlation function which defines the conductivity of the system via the standard Kubo formula.[12] Damping is introduced by dressing the Green's-function propagators by the relevant acoustic-phonon self-energies. The factor $(1-\cos\theta)$ is associated with the corresponding vertex corrections consisting of ladder diagrams which are required in order to obey the Ward identities.[13,14] As a result of the $(1-\cos\theta)$ factor in the integrand for τ_t^{-1}, we see that it is the large-angle scattering events which contribute significantly to the relaxation rate. Small-angle scattering events where $\cos\theta\approx 1$ make a negligible contribution to τ_t^{-1} as one qualitatively expects since such events hardly impede the electrons.

D. Transport in the Bloch-Grüneisen regime

In our discussion thus far, we have considered the quasielastic scattering of electrons from acoustic phonons in the EP regime where $\hbar\omega_Q \ll k_BT$. In this section we obtain the relaxation times for lower temperatures in the BG regime where $\hbar\omega_Q\approx k_BT$. The fact that the acoustic-phonon energies are comparable to k_BT gives rise to a new, more complicated temperature dependence of the relaxation rates via the statistical occupation factors.[15,16] At low enough temperatures acoustic phonons with wave vector $q\approx 2k_F$ cease to be appreciably excited, and no longer contribute to the relaxation rate. In the vicinity of the Fermi energy, only phonons with small wave vectors can contribute to the scattering rate. The transition into the BG regime roughly occurs at a temperature given by $k_BT_{\rm BG}\approx 2k_F\hbar u_l$. For $n_s=(1$ and $6)\times 10^{11}$ cm^{-2}, the transition temperature $T_{\rm BG}=6.22$ and 15.25 K, respectively.[5,15,16] The transition into the BG regime is characterized by a dramatic decrease in the relaxation rate for $E\approx E_F$, and correspondingly we expect a stronger dependence of the reciprocal mobility on T.

In the BG regime instead of the EP form for $\Delta(E,E')$, we keep the full form as in Eq. (20). We still assume quasielasticity so that we still obtain closed-form solutions for the relaxation rates:

$$\tau_j^{-1}(E)=\frac{m^*}{\hbar^3}\frac{4}{(2\pi)^2}\int_0^{\pi}d\alpha(1-\cos\theta)\int_0^{\infty}dq_z|I(q_z)|^2\frac{|C_j(q,q_z)|^2}{\epsilon^2(q,T)}$$
$$\times\frac{1}{[1-f_0(E)]}\{N_Q[1-f_0(E+\hbar\omega_Q)]+(N_Q+1)[1-f_0(E-\hbar\omega_Q)]\}\ , \tag{39}$$

where the C_j's are given by Eqs. (18a)–(18c). In the limit $\hbar\omega_Q/k_BT\ll 1$, these relaxation rates approach the equipartition results given in Eqs. (30a)–(30c). The drift mobility in the BG regime can then be evaluated using Eqs. (36) and (38).

E. Transport in the inelastic regime

As the temperature of the 2DEG is raised above $T\approx 40$ K, the scattering from polar LO phonons starts to dominate the transport properties of the 2DEG. The previous simplifications in the evaluation of the perturbation distribution intimately associated with the quasielastic approximation are no longer valid. For inelastic processes, $\phi(E)$ is no longer obtainable in a simple closed form. In particular, the solution is not given by simply multiplying the inelastic LO-phonon scattering rate by $(1-\cos\theta)$. If inelastic processes are involved, the linearized Boltzmann equation must be solved directly.

The matrix element for scattering from bulk polar LO phonons is given by[6,7]

$$|C_{\rm LO}(Q)|^2=\frac{2\pi e^2\hbar\omega_0}{Q^2}\left[\frac{1}{\epsilon_\infty}-\frac{1}{\epsilon_0}\right]\ , \tag{40}$$

where $\hbar\omega_0=36.8$ meV is the LO-phonon energy, and $\epsilon_\infty=10.92$ is the optical dielectric constant in GaAs. Assuming the LO phonons to be dispersionless, using Eqs. (14)–(16), (27), and (40), we obtain the 2D differential scattering rate

$$S_{\rm II}(\mathbf{k},\mathbf{k}')=\frac{e^2\omega_0}{2q}\left[\frac{1}{\epsilon_\infty}-\frac{1}{\epsilon_0}\right]H(q)\Delta(E,E')\ , \tag{41}$$

where $\Delta(E,E')$ is given by Eq. (20) with $\hbar\omega_Q=\hbar\omega_0$, independent of the 3D phonon wave vector Q. The corresponding collision integral for LO-phonon scattering in a 2DEG is

$$I_c[f]=-\frac{e\hbar F}{m^*}\frac{\partial f_0}{\partial E}k\cos\theta\frac{e^2\omega_0}{2}\left[\frac{1}{\epsilon_\infty}-\frac{1}{\epsilon_0}\right]\frac{1}{1-f_0(E)}$$
$$\times\int d^2k'\left[\phi(E)-\frac{k'\cos\theta}{k}\phi(E')\right][1-f_0(E')]\frac{H(q)}{q}\Delta(E,E')\ . \tag{42}$$

For a frequency of ω_0 we assume screening effects to be small and ignore them; otherwise the problem would require a dynamical screening calculation.

Substituting Eq. (42) into Eq. (3), the 2D Boltzmann equation can be written in the form of a difference equation coupling $\phi(E)$ with $\phi(E\pm\hbar\omega_0)$,[4,3]

$$1=S_0(E)\phi(E)-S_a(E)\phi(E+\hbar\omega_0)-S_e(E-\hbar\omega_0)\phi(E-\hbar\omega_0)\ , \tag{43}$$

where $S_0(E)$ denotes the sum of the in-scattering and out-scattering contributions of the quasielastic processes due to acoustic phonons, and the out-scattering contribution from the LO phonons. The other terms $S_a(E)$ and $S_e(E)$ denote the in-scattering contributions from the inelastic-scattering processes due to the LO phonons. After some algebra we obtain

$$S_0(E)=\frac{m^*\omega_0e^2}{b\hbar^2}\left[\frac{1}{\epsilon_\infty}-\frac{1}{\epsilon_0}\right]\frac{1}{1-f_0(E)}\{N_0[1-f_0(E+\hbar\omega_0)]I^+(E)$$
$$+(N_0+1)[1-f_0(E-\hbar\omega_0)]I^-(E)\}+\frac{1}{\tau_{\rm tot}(E)}\ , \tag{44a}$$

$$S_a(E)=\frac{m^*\omega_0e^2}{b\hbar^2}\left[\frac{1}{\epsilon_\infty}-\frac{1}{\epsilon_0}\right]\frac{1}{1-f_0(E)}\left[N_0[1-f_0(E+\hbar\omega_0)]\left[\frac{E+\hbar\omega_0}{E}\right]^{1/2}J^+(E)\right]\ , \tag{44b}$$

$$S_e(E)=\frac{m^*\omega_0e^2}{b\hbar^2}\left[\frac{1}{\epsilon_\infty}-\frac{1}{\epsilon_0}\right]\frac{1}{1-f_0(E)}\left[(N_0+1)[1-f_0(E-\hbar\omega_0)]\Theta(E-\hbar\omega_0)\left[\frac{E-\hbar\omega_0}{E}\right]^{1/2}J^-(E)\right]\ , \tag{44c}$$

where $1/\tau_{\rm tot}(E)$ is given by Eq. (38), $N_0=1/[\exp(\beta\hbar\omega_0)-1]$, and the angular integrals $I^{\pm}(E)$ and $J^{\pm}(E)$ are given by

$$I^{\pm}(E)=\int_0^{\pi} d\theta \left[\frac{1+(\frac{9}{8})u_{\pm}(E,\theta)+(\frac{3}{8})u_{\pm}^2(E,\theta)}{u_{\pm}(E,\theta)[1+u_{\pm}(E,\theta)]^3} \right] \tag{45a}$$

and

$$J^{\pm}(E)=\int_0^{\pi} d\theta \cos\theta \left[\frac{1+(\frac{9}{8})u_{\pm}(E,\theta)+(\frac{3}{8})u_{\pm}^2(E,\theta)}{u_{\pm}(E,\theta)[1+u_{\pm}(E,\theta)]^3} \right] . \tag{45b}$$

The functions $u_{\pm}(E,\theta)$ are defined by

$$u_{\pm}(E,\theta)=\left[\frac{2m^*}{\hbar^2 b^2}[2E\pm\hbar\omega_0-2\sqrt{E(E\pm\hbar\omega_0)}\cos\theta] \right]^{1/2} . \tag{46}$$

A great deal of literature on solving Eq. (43) in bulk systems exists when the relaxation-time approximation is no longer valid. Many techniques have been applied such as the variational, matrix, and Monte Carlo methods.[17] The most sophisticated theoretical work in this regime has been carried out by Vinter,[18,19] who uses numerical wave functions and includes the effect of multisubbands and solves the Boltzmann equation by a combination of matrix and iterative techniques. In this paper we adopt the iteration method first formulated by Rode.[20–22] For a given value of the electron energy $E=E_i+l\hbar\omega_0$, where $0<E_i<\hbar\omega_0$ and $l=0,1,2\ldots$, we set $S_a(E)=S_e(E)=0$ so that the zeroth-order solution of $\phi(E_i+l\hbar\omega_0)$ are given by

$$\phi^{(0)}(E_i+l\hbar\omega_0)=S_0^{-1}(E_i+l\hbar\omega_0) , \tag{47a}$$

$$\phi^{(0)}(E_i+(l\pm1)\hbar\omega_0)=S_0^{-1}(E_i+(l\pm1)\hbar\omega_0) . \tag{47b}$$

By repeatedly carrying out a Ritz iteration of Eq. (43), it follows that in the $(n+1)$th iteration we have that[4,3]

$$\begin{aligned}\phi^{(n+1)}(E_i+l\hbar\omega_0)=S_0^{-1}(E_i+l\hbar\omega_0)[1+S_a(E_i+l\hbar\omega_0)\phi^{(n)}(E_i+(l+1)\hbar\omega_0)\\ +S_e(E_i+l\hbar\omega_0)\phi^{(n)}(E_i+(l-1)\hbar\omega_0)] .\end{aligned} \tag{48}$$

The iteration is terminated for a given value of E when $\phi^{(n+1)}(E)$ converges to within some preset tolerance. Note that in this method degeneracy is properly taken into account, and we completely bypass the use of Matthiessen's rule. Once the values of $\phi(E)$ are obtained in this way, the mobility can be calculated from Eqs. (35) and (36), with $\tau(E)$ replaced by $\phi(E)$.

Although strictly speaking no closed-form expression exists for the perturbation distribution when inelastic-scattering processes are involved, a relaxation time may be obtained within certain approximations. For the case of low temperatures the in-scattering term via phonon absorption $S_a(E)$ is negligible due to the scarcity of phonons with energy $\hbar\omega_0$, and the corresponding emission term $S_e(E)$ is negligible since there are only a few electrons with a phonon quantum of energy.[20] Therefore, at low enough temperatures it is justified to ignore the in-scattering terms in determining $\phi(E)$, which gives us the low-temperature relaxation-time approximation

$$\tau_{\rm LT}(E)=S_0^{-1}(E) . \tag{49}$$

If the electron energy E is much larger than $\hbar\omega_0$, as is the case at high temperatures, we can make the replacement $\phi(E\pm\hbar\omega_0)\rightarrow\phi(E)$, and we arrive at the high-energy relaxation-time approximation

$$\tau_{\rm HE}(E)=\frac{1}{S_0(E)-S_a(E)-S_e(E)} . \tag{50}$$

The relaxation times $\tau_{\rm LT}$ and $\tau_{\rm HE}$ are simply the 2D version of the Fröhlich relaxation-time approximations[23,24,3] for LO-phonon scattering, including the quasielastic scattering from acoustic phonons.

III. RESULTS AND DISCUSSION

A. Relaxation and scattering rates in the equipartition regime

Using the theoretical model outlined in the preceding section we calculate the scattering rates τ_s^{-1} and relaxation rates τ_t^{-1} due to acoustic phonons, as a function of the electron energy E, in the EP regime. The relevant rates have been obtained in Eqs. (30a)–(30c). Our result for the individual DP and total PE rates are given in Figs. 1(a)–1(d), for $n_s=1\times10^{11}$ and 6×10^{11} cm^{-2}, at two different temperatures $T=20$ and 40 K. We take $D=12$ eV and set the depletion density to $n_{\rm depl}=5\times10^{10}$ cm^{-2}. Unlike the case for scattering from remote ionized impurities[12] where the transport relaxation time τ_t can be greater than the scattering time τ_s by orders of magnitude, due to the long-range nature of the electron-impurity interaction, we see that $\tau_t/\tau_s\approx1$, since the screened electron–acoustic-mode phonon interactions are of relatively short range.

Using Eq. (35) for the drift mobility we calculate the reciprocal of the acoustic-phonon limited mobility as a function of temperature for different values of the deformation-potential constant in Fig. 2, and different

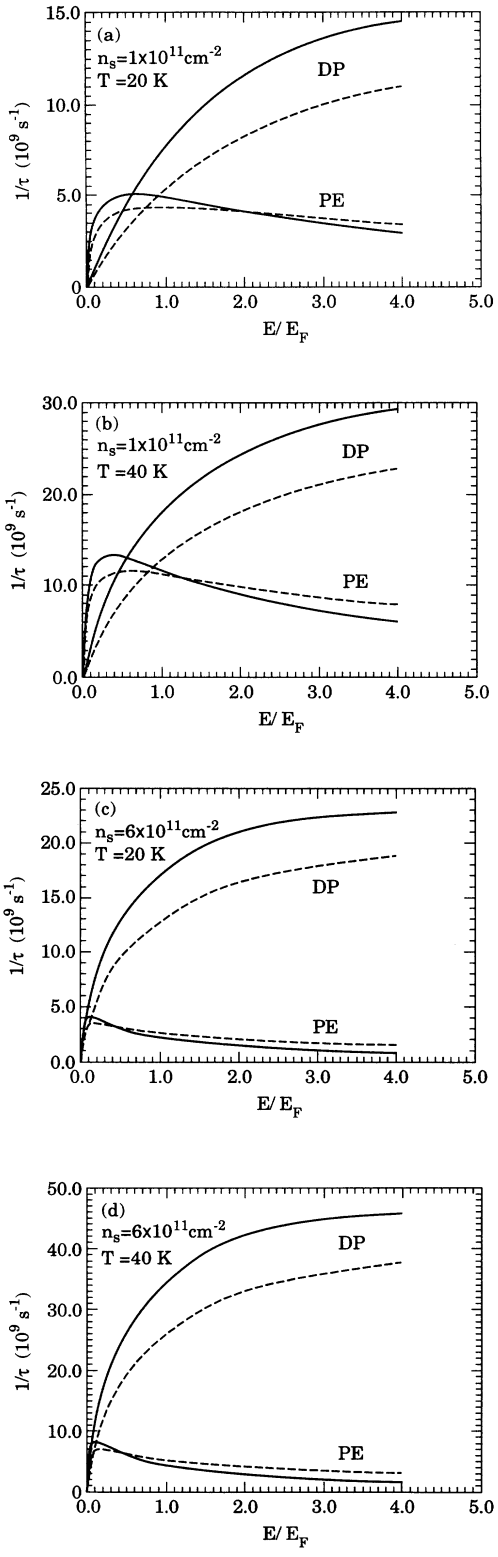

FIG. 1. The relaxation rate $\tau_t(E)$ (solid line) and scattering rate $\tau_s(E)$ (dashed line) in the equipartition regime as a function of electron energy E for different densities and temperatures. (a) $n_s=1\times10^{11}$ cm^{-2} and $T=20$ K; (b) $n_s=1\times10^{11}$ cm^{-2} and $T=40$ K; (c) $n_s=6\times10^{11}$ cm^{-2} and $T=20$ K; (d) $n_s=6\times10^{11}$ cm^{-2} and $T=40$ K. In (a)–(d) we take $D=12$ eV and $n_{\rm depl}=5\times10^{10}$ cm^{-2}.

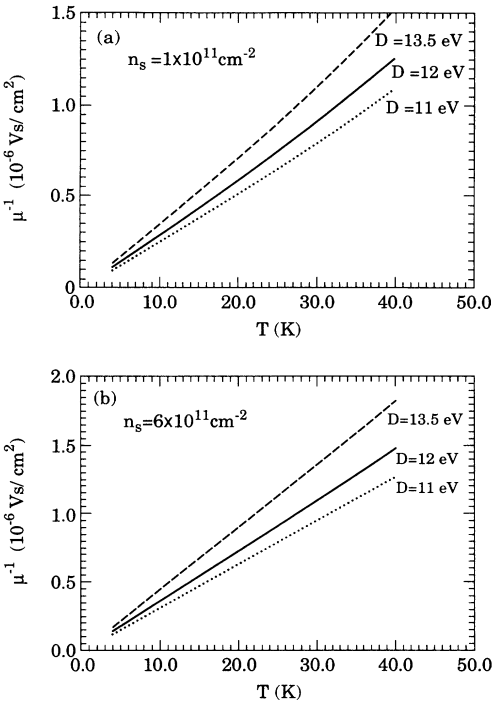

FIG. 2. Temperature dependence of the reciprocal mobility limited by acoustic phonons $\mu_{\rm ac}$ for three different values of the deformation-potential constant D. (a) $n_s=1\times10^{11}$ cm^{-2} and (b) $n_s=6\times10^{11}$ cm^{-2} $D=11$ eV (dotted line), $D=12$ eV (solid line), $D=13.5$ eV (dashed line), and $n_{\rm depl}=5\times10^{10}$ cm^{-2}.

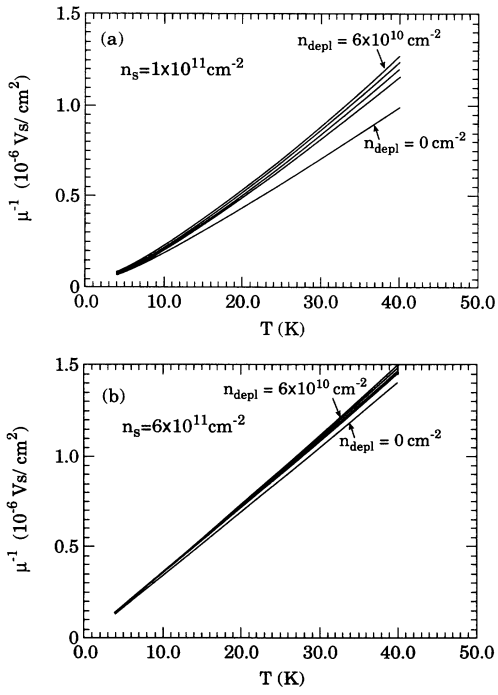

FIG. 3. Temperature dependence of the reciprocal mobility limited by acoustic phonons $\mu_{\rm ac}$ for different values of the depletion density $n_{\rm depl}=(0.0,3.0,4.0,5.0,6.0)\times10^{10}$ cm^{-2} for carrier densities (a) $n_s=1\times10^{11}$ cm^{-2} and (b) $n_s=6\times10^{11}$ cm^{-2}. The uppermost cases in both (a) and (b) correspond to the highest value of $n_{\rm depl}$.

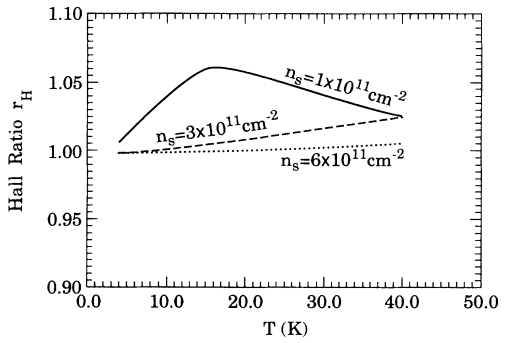

FIG. 4. The Hall ratio r_H as a function of temperature T for three different carrier densities for $D=12$ eV, and $n_{\text{depl}}=5\times10^{10}$ cm^{-2}. $n_s=1\times10^{11}$ cm^{-2} (solid line); $n_s=3\times10^{11}$ cm^{-2} (dashed line); $n_s=6\times10^{11}$ cm^{-2} (dotted line).

values of the depletion density in Fig. 3. As expected, the mobility for fixed T decreases with increasing D and n_{depl}.

From Eq. (37) for the relevant averaging over the carrier distribution for the Hall mobility μ_H, we evaluate the dimensionless Hall ratio $r_H=\mu_D/\mu_H$ as a function of T for three different densities $n_s=(1,3,6)\times10^{11}$ cm^{-2} in

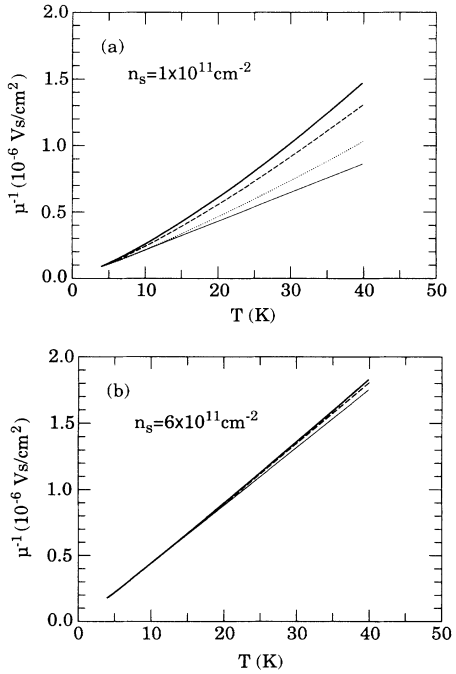

FIG. 5. Temperature dependence of the reciprocal mobility for two different electron sheets densities. (a) $n_s=1\times10^{11}$ cm^{-2} and (b) $n_s=6\times10^{11}$ cm^{-2}. The results given by the thick solid lines include temperature-dependent screening and thermal averaging over energy. The dashed lines represent calculations which do not have the averaging over energy. The dotted lines represent calculations which ignore the temperature dependence of screening. The thin lines correspond to calculations without any temperature-dependent effects. In (b) the dotted line coincides with the thin line. $n_{\text{depl}}=5\times10^{10}$ cm^{-2} and $D=13.5$ eV.

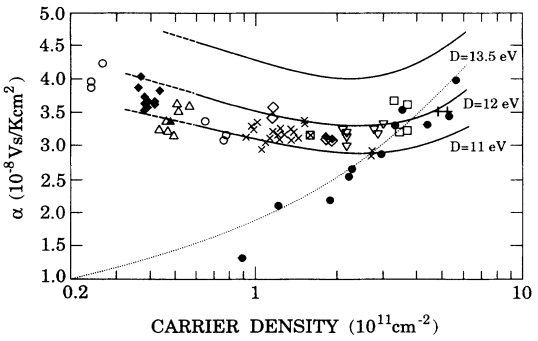

FIG. 6. Linear coefficient of the temperature dependence α as a function of the electron sheet density n_s. The solid lines are the theoretical curves for three different values of the deformation-potential constant D. These curves are extrapolated to lower densities by the dashed lines. The dotted line is the theoretical curve for $D=13.5$ eV, for a vanishing depletion density without any temperature-dependent effects. Results reported by Mendez, Price, and Heiblum (Ref. 27) are plotted by ●; other data points are from Harris *et al.* (Ref. 43).

the temperature range $T=4$–40 K. For $n_s=1\times10^{11}$ cm^{-2} the Hall ratio exhibits a maximum of ≈1.07 for $T\approx15.5$. We see from Fig. 4 that for the density and EP temperature range investigated in this paper, $r_H\approx1$.

In the following section we discuss the way in which the fundamental coupling constants for the

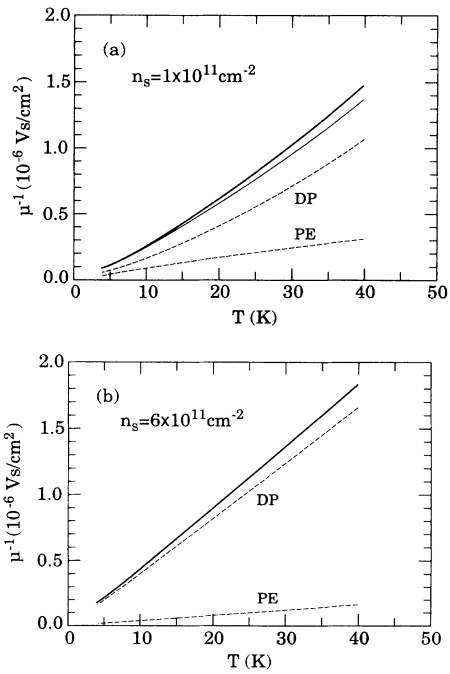

FIG. 7. Temperature dependence of the reciprocal mobility for two different electron sheet densities (a) $n_s=1\times10^{11}$ cm^{-2} and (b) $n_s=6\times10^{11}$ cm^{-2}. Results given by the dashed lines are for the deformation-potential and piezoelectric-coupled acoustic mode phonons. Their sum is given by the solid lines; its discrepancy from the thick solid lines shows the departure from Matthiessen's rule. In (b) the thin and thick solid lines coincide. $n_{\text{depl}}=5\times10^{10}$ cm^{-2} and $D=13.5$ eV.

electron–acoustic-phonon interaction are determined from the transport properties.

B. Temperature dependence of low-temperature mobility

For carrier densities $n_s=(1.0-6.0)\times10^{11}$ cm^{-2} it is experimentally observed that in the EP temperature range $T\approx4-40$ K the reciprocal mobility increases linearly with temperature,

$$\frac{1}{\mu}=\frac{1}{\mu_0}+\alpha T \ . \tag{51}$$

The slope α increases with n_s independently of the zero-temperature mobility μ_0, for high-mobility samples with $\mu_0>10^5$ cm^2/V s. In a typical $Al_xGa_{1-x}As/GaAs$ modulation-doped semiconductor the electron wave function is mainly confined in GaAs so that the influence of alloy disorder scattering can be considered negligible. Interface-roughening scattering also plays a minor role due to the smoothness of the interface in high-quality heterojunctions.[25] In this section we investigate in detail the contributing factors to the linear coefficient α of the temperature dependence in the EP regime.

If the scattering from ionized impurities is independent of the temperature[26] in ultrahigh-mobility samples for $T<40$ K the need to quantify the ionized impurity scattering is eliminated, so that the temperature dependence of μ can solely be attributed to the acoustic phonons. Adopting the theoretical model outlined in the preceding section, a reasonable agreement of the temperature dependence of μ with experimental results[27–30,1] is obtained only by assuming a value of $D=12-13.5$ eV, which is significantly greater than the generally accepted value[31] in bulk GaAs ($D=7$ eV). Some other studies which completely or partly ignore screening effects,[32–34] suggest that the temperature dependence of μ is satisfactorily explained using a value of $D=7-8$ eV. Undoubtedly, the extensive investigation of the mobility in a 2DEG is partly motivated by the controversy surrounding the exact value of the DP constant in GaAs.[35–37]

Enhanced values of D have also been independently inferred from an analysis of energy relaxation data in GaAs heterojunctions.[38–40] We comment here that in the power loss context there exists a possibility that the value of the DP constant may be reconciled with its bulk value. By including the contribution of the low-energy phonon modes associated with the coupling of quasiparticle excitations to the LO phonons[41] to the total average energy loss via acoustic phonons,[40] good agreement with experi-

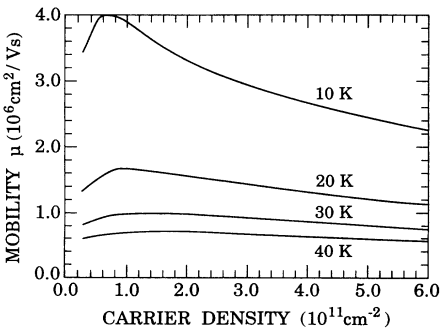

FIG. 8. The acoustic-phonon limited mobility μ_{ac} plotted as a function of the carrier density n_s for four different temperatures. $n_{depl}=5\times10^{10}$ cm^{-2} and $D=12$ eV.

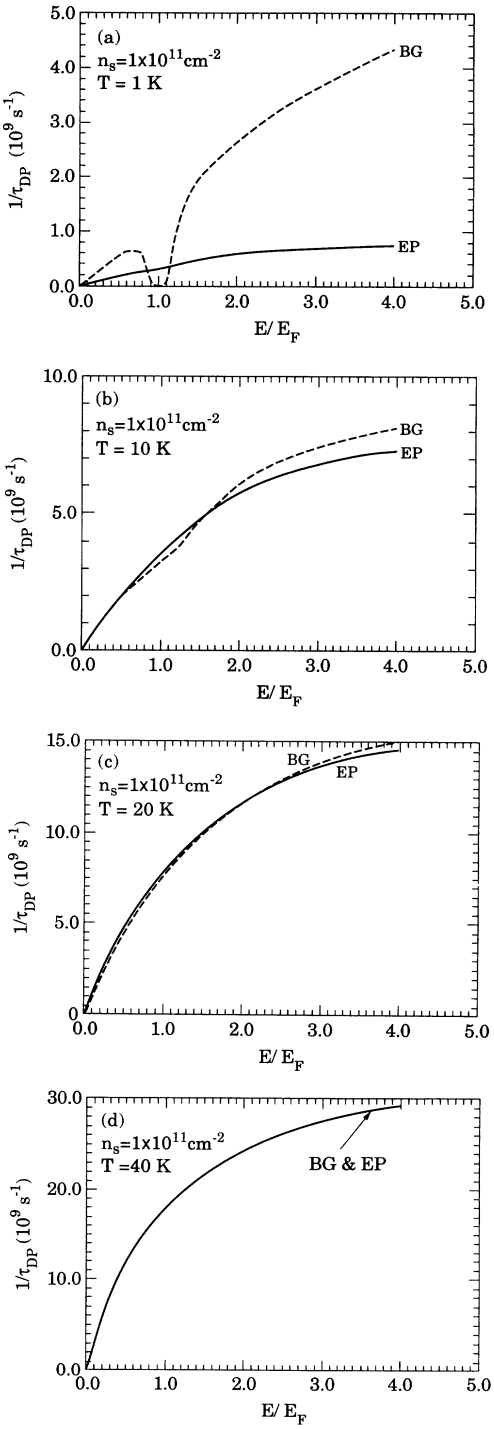

FIG. 9. The equipartition (solid line) and Bloch-Grüneisen (dashed line) deformation-potential relaxation rate $\tau_{DP}^{-1}(E)$ for a carrier density $n_s=1\times10^{11}$ cm^{-2} at different temperatures; (a) $T=1$ K, (b) $T=10$ K, (c) $T=20$ K, and (d) $T=40$ K. $D=12$ eV and $n_{depl}=5\times10^{10}$ cm^{-2}.

mental data is obtained[42] at low temperatures with $D=7$ eV.

A claim has also been made that the PE coupling constant is also enhanced in heterolayers.[43] Harris *et al.*[43] study the acoustic-phonon-scattering process in ultrahigh-mobility GaAs heterojunctions over a much wider range of carrier densities than in previous works. In their ultrapure samples, scattering by both remote and background ionized impurities is significantly reduced so that the temperature dependence of μ of $T\approx 4-40$ K is expected to be dominated by acoustic phonons.[43,29] For low electron densities, n_s below $\approx 2\times 10^{11}$ cm^{-2}, they find that a simple extrapolation of the existing theoretical models[5,37] does not show good agreement with their experimental results (see Fig. 6). Their measured values of α are clearly larger than the extrapolated theoretical results at lower carrier densities. They suggest that the discrepancy arises from the fact that the piezoelectric constant h_{14} in a 2DEG is $\approx 50\%$ greater than in bulk GaAs. We find, consistent with earlier claims,[29,28,27] that to explain the experimental results of Ref. 42, one requires an enhanced value of D, but our calculations clearly show that a corresponding *ad hoc* enhancement of h_{14} to explain the low-density data is unnecessary.[44] We find that the temperature-dependent effects arising from screening and thermal averaging over the carrier distribution become increasingly important at lower densities, and it is incorrect to simply extrapolate the high-density results which do not include these temperature-dependent effects. For high carrier densities above $\approx 2\times 10^{11}$ cm^{-2}, the temperature dependence of screening in the temperature range 4–40 K is rather negligible, and the static polarizability $\Pi(q,T)=\Pi_0(q)$ is simply the zero-temperature polarizability function for the 2DEG as given in Eq. (25), calculated in the RPA. For low values of n_s, the temperature dependence of $\Pi(q,T)$ becomes rather significant. As T increases, $\Pi(q,T)$ for $q\approx 2k_F$ decreases, thereby reducing the effect of screening by the 2DEG and increasing the value of the acoustic-phonon limited mobility $\mu_{\rm ac}$.

We numerically evaluate μ_{ac} in the temperature range $T\approx 4-40$ K for a range of carrier densities $n_s=(0.3-6.0)\times 10^{11}$ cm^{-2}. We keep both the temperature dependence of screening and the effect of thermal smearing of the electron energy [see Eqs. (24) and (36)]. We also estimate their relative importance at various densities. If both the temperature-dependent effects in the evaluation of $\langle \tau(E)\rangle$ are suppressed,[5] it follows from the equipartition of electron-phonon scattering that $\mu_{\rm ac}^{-1}$ is *strictly* linearly proportional to T. The crucial point is that an approximate linear dependence is preserved even in the presence of these two effects in the temperature and density range of interest in this section.

The combined and isolated effects of the temperature dependence of $\mu_{\rm ac}^{-1}(T)$ are shown in Fig. 5 for $n_s=1\times 10^{11}$ and 6×10^{11} cm^{-2}. The solid lines represent the theoretical calculations which include both the temperature-dependent screening and thermal averaging over the distribution, whereas the thin solid lines exclude both effects and are, therefore, strictly linear in T. As expected, at the higher density $n_s=6\times 10^{11}$ cm^{-2}, the temperature-dependent effects are not very significant. At high n_s, thermal averaging over energy is completely negligible and the effect of the temperature dependence of screening is noticeable only at higher temperatures $T>20$ K. At the lower density, both temperature-dependent effects are rather important, with the temperature-dependent screening effect being stronger than the thermal averaging effect.

We make a linear fit of the thick solid lines (which include both temperature-dependent effects) in the temperature range $T=20-40$ K, where we expect EP to be valid, and identify its slope with the experimentally measured temperature coefficient, $\alpha=d\mu_{\rm ac}^{-1}(T)/dT$. The results of our theoretical calculation of $\alpha(n_s)$ for the density range $n_s=(0.6-6.0)\times 10^{11}$ cm^{-2} are given in Fig. 6 for three different values of D. Assuming a value $n_{\rm depl}=5\times 10^{10}$ cm^{-2} for the depletion density, the optimal value for D is slightly less than 12 eV. We extrapolate the results down to lower densities by the dashed lines, since for small $n_s/n_{\rm depl}$ ratios the variational wave function may not be sufficiently accurate.[45] Although the theoretical curve for $\alpha(n_s)$ which ignores both temperature-dependent effects agrees fairly well with the experimental data at high densities above $n_s\approx 3\times 10^{11}$ cm^{-2}, the fit becomes increasingly poor at lower densities. The temperature dependences arising from screening and thermal averaging significantly augment $\mu_{\rm ac}^{-1}$ at high temperatures, increasing the temperature coefficient α as the density is decreased, giving rise to the nonmonotonic behavior of $\alpha(n_s)$ seen in Fig. 6. Our claim is that this explains the rather curious minimum in $\alpha(n_s)$ observed in the experimental data of Harris *et al.*[43]

In Fig. 7 we show the individual temperature dependences of the reciprocal mobility limited by the deformation-potential and piezoelectric-coupled acoustic-mode scattering. Their sum is compared to the total acoustic-phonon-scattering-limited mobility to check the validity of Matthiessen's rule. (A similar analysis was carried out by Stern[46] for silicon inversion layers including Coulomb and surface-roughness scattering.) At high densities and low temperatures, Matthiessen's rule holds extremely well, but at low densities and high temperatures it does not work as well (where we observe the expected inequality), although the effect on α is small (less than 10%). Finally in Fig. 8 we show the density dependence of the acoustic-phonon-scattering-limited mobility itself for four different temperatures. The maximum in $\mu_{\rm ac}(n_s)$ for a given temperature arises from a competition between the screening effect which dominates at lower n_s (and tends to increase $\mu_{\rm ac}$ with increasing n_s), and the matrix element effect which dominates at higher n_s (and tends to decrease with $\mu_{\rm ac}$ with increasing n_s). Both of these effects go down with increasing temperature, producing a very weak density-dependent $\mu_{\rm ac}$ at higher T. We point out that the results shown in Fig. 8 apply only when impurity scattering has been *completely* eliminated. In real systems there will be an additional n_s dependence of μ arising from

screening effects associated with the charged impurity scattering.

C. Relaxation rate and mobility in the Bloch-Grüneisen regime

We compare the BG relaxation rate Eq. (39) with the EP rate Eq. (28) for the DP coupled scattering by acoustic phonons in Figs. 9 and 10 for $n_s=(1 \text{ and } 6)\times 10^{11}$ cm^{-2} for temperatures $T=1$, 10, 20, and 40 K. The BG and EP results tend to diverge as the temperature is lowered. In particular, the BG relaxation rate shows a characteristic dip in a narrow region around the Fermi energy E_F. Comparing Figs. 9(a)–9(d) and 10(a)–10(d), we see as expected that the transition into the BG regime manifests itself in the relaxation time τ_t^{-1} at a higher temperature for higher densities, in accordance with the rough estimates of T_{BG} given earlier. The same general features are exhibited for the BG and EP relaxation rates for the piezoelectric-coupled scattering, as can be seen in Figs. 11(a)–11(d).

For $n_s=(1 \text{ and } 6)\times 10^{11}$ cm^{-2}, we calculate the mobility in the BG regime which is plotted in Fig. 12, and compare it with the EP results of the preceding section. The reciprocal mobilities as determined by the BG relaxation rates are shifted downwards slightly from the EP curves since EP tends to overestimate the Bose factor for acoustic phonons. We observe the characteristic stronger dependence of μ_{ac}^{-1} on T at low temperatures especially at higher densities as shown in Fig. 13(a). At high temperatures the expected quasilinear behavior of the EP regime is recovered. For low temperatures we extract the effective exponent γ for the temperature dependence of the reciprocal mobilities T^{γ} from the log-log plot in Fig. 13(b) for densities $n_s=(1-10)\times 10^{11}$ cm^{-2}. It is clearly evident from this graph that μ_{ac}^{-1} enters into the strongly T-dependent BG regime at higher temperatures for higher densities n_s. By employing a linear fit of the low-temperature portion of the curves we obtain the following values for the effective exponent γ. For $n_s=(4-10)\times 10^{11}$ cm^{-2}, we have that $\gamma\approx 4.5$. As the density is lowered, the value of γ decreases slightly for the particular temperature range under investigation. We obtain $\gamma=4.3$, 4.0, and 3.2 for densities $n_s=(3,2,1)\times 10^{11}$ cm^{-2}, respectively. We conclude that the asymptotic value of γ in this model is probably $\gamma\approx 4.5$. Using a power counting method based on the strong screening approximation and Matthiessen's rule, and setting the perpendicular Fourier transform of the electron density to unity for small q_z, it is easy to show[15] that the reciprocal mobility becomes the sum $\mu_{ac}^{-1}=c_1T^7+c_2T^5$. The relevant prefactors have been derived by Störmer *et al.*,[16] who have experimentally observed the transition into the BG regime. Our results for the lower densities (especially for $n_s=1\times 10^{11}$ cm^{-2}) indicate that the transition into the BG regime has not been fully completed even for temperatures as low as $T=1$ K. For $T<1$ K, however, the overall temperature dependence of mobility (in ultrapure heterojunctions) is extremely weak (and the background impurities in GaAs

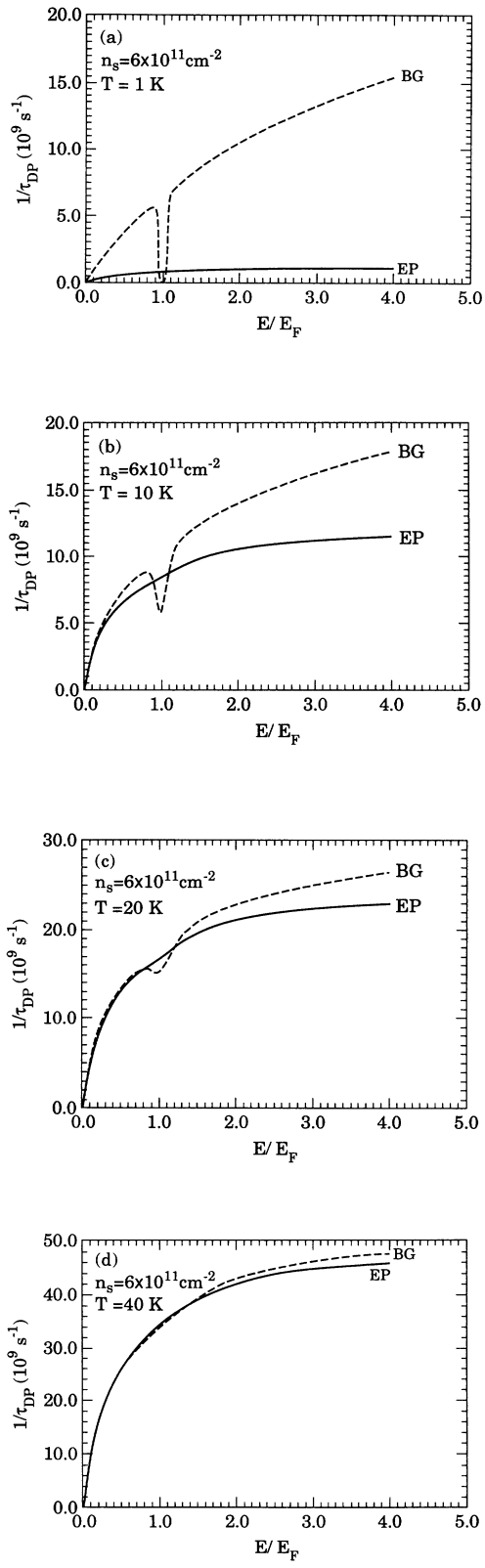

FIG. 10. The equipartition (solid line) and Bloch-Grüneisen (dashed line) deformation-potential relaxation rate $\tau_{DP}^{-1}(E)$ for a carrier density $n_s=6\times 10^{11}$ cm^{-2} at different temperatures: (a) $T=1$ K, (b) $T=10$ K, (c) $T=20$ K, and (d) $T=40$ K. $D=12$ eV and $n_{depl}=5\times 10^{10}$ cm^{-2}.

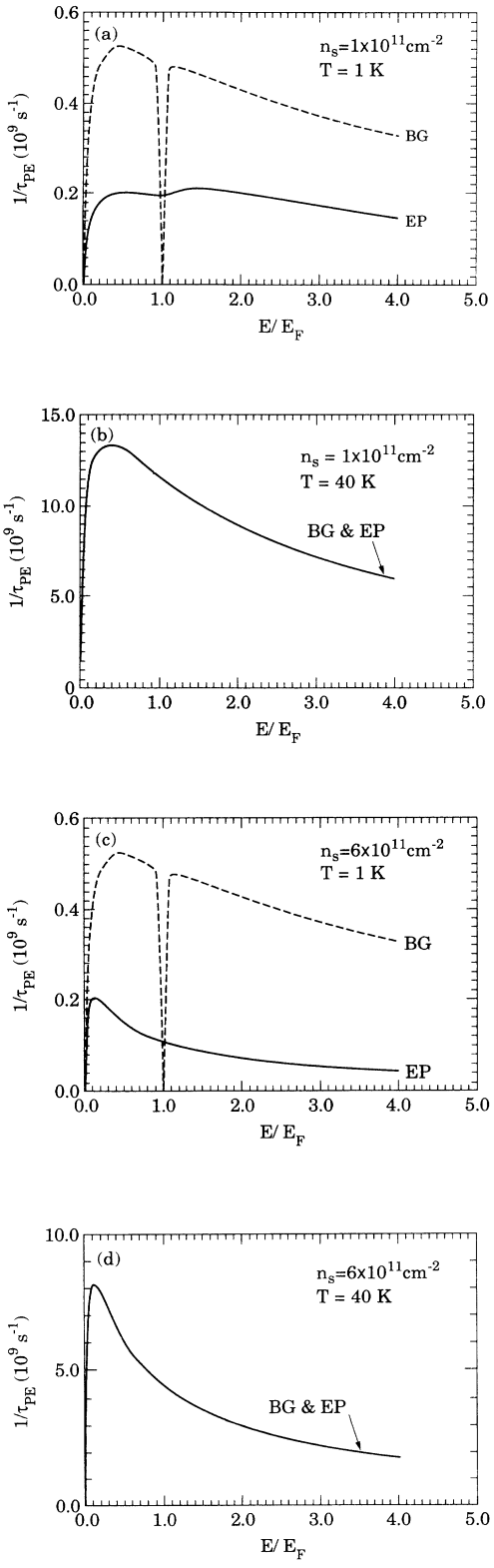

FIG. 11. The equipartition (solid line) and Bloch-Grüneisen (dashed line) total piezoelectric relaxation rate $\tau_{PE}^{-1}(E)$ for different densities and temperatures: (a) $n_s=1\times10^{11}$ cm^{-2}, $T=1$ K; (b) $n_s=1\times10^{11}$ cm^{-2}, $T=40$ K; (c) $n_s=6\times10^{11}$ cm^{-2}, $T=1$ K; and (d) $n_s=6\times10^{11}$ cm^{-2}, $T=40$ K. $D=12$ eV and $n_{depl}=5\times10^{10}$ cm^{-2}.

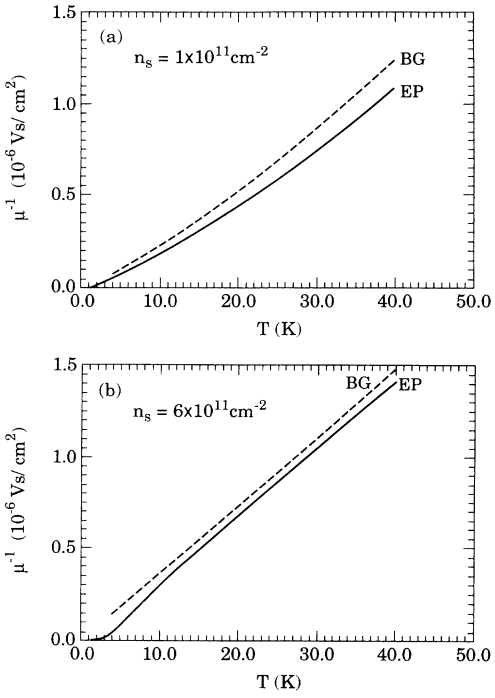

FIG. 12. The mobility limited by acoustic-phonon scattering using the Bloch-Grüneisen (solid line) and equipartition (dashed line) relaxation rates. (a) $n_s=1\times10^{11}$ cm^{-2}, (b) $n_s=6\times10^{11}$ cm^{-2}. $D=12$ eV and $n_{depl}=5\times10^{10}$ cm^{-2}.

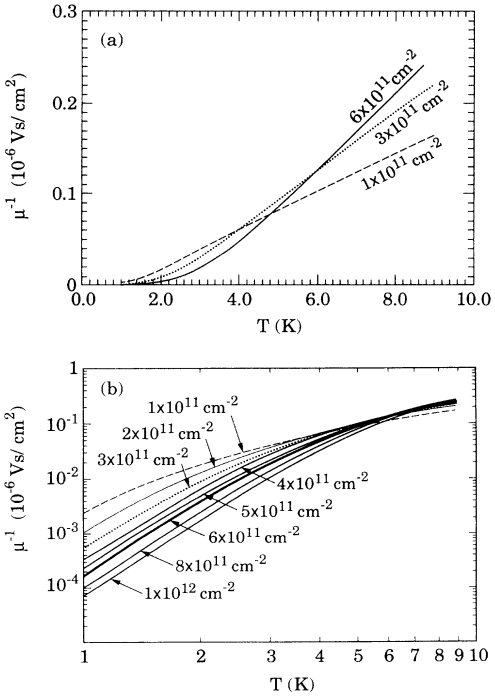

FIG. 13. The temperature dependence of the low-temperature Bloch-Grüneisen mobility for (a) densities $n_s=(1,3,6)\times10^{11}$ cm^{-2} on a linear plot, and (b) densities $n_s=(1-10)\times10^{11}$ cm^{-2} on a log-log plot. $D=12$ eV and $n_{depl}=5\times10^{10}$ cm^{-2}.

most likely contribute to this temperature dependence). For this reason we did not extend our calculation below 1 K.

D. Perturbation distribution function and mobility in the inelastic regime

We solve for the scattering rate $\phi(E)$ by an iterative procedure as described in Sec. II. In Figs. 14(a)–14(c) and 15(a)–15(c) we show the perturbation distribution $\phi^{-1}(E)$ for $n_s=(1 \text{ and } 6)\times 10^{11}$ cm^{-2} at $T=20$ and 300 K. For low temperatures we see that $\phi^{-1}(E)$ coincides with the EP result for the relaxation rate due solely to acoustic phonons and with the low-temperature and high-energy relaxation rate approximations exactly over that portion of carrier energies which determines the transport coefficients of the 2DEG [see Figs. 14(b) and 15(b)]. However, as T is increased the distribution is no longer degenerate and a larger energy range is sampled for the thermal averaging necessary to determine the transport properties. In this case [see Figs. 14(c) and 15(c)] the oscillatory bumps in the perturbation distribution $\phi^{-1}(E)$ start to contribute, and an appreciable reduction in the mobility takes place. The oscillatory behavior is due to the fact that $\phi(E)$ is coupled to $\phi(E\pm\hbar\omega_0)$. We note that the high-energy relaxation rate $\tau_{\rm HE}^{-1}$ approaches the iteration result for large E. A comparison of the mobility limited by LO and acoustic phonons calculated via the iterative scheme and the closed-form relaxation rate

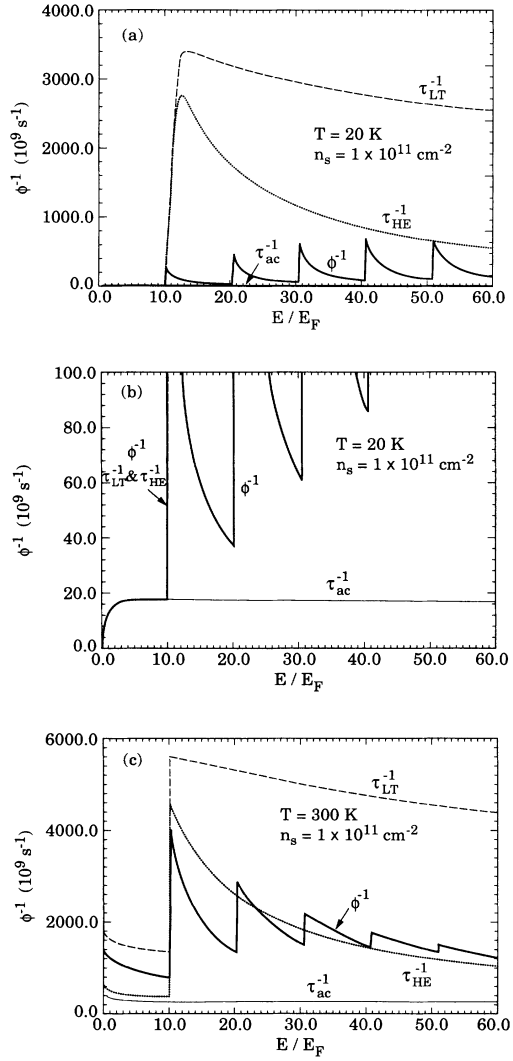

FIG. 14. The perturbation function $\phi^{-1}(E)$ (thick solid line), low-temperature relaxation rate $\tau_{\rm LT}^{-1}$ (dashed line), and high-energy relaxation rate $\tau_{\rm HE}^{-1}$ (dotted line) due to quasielastic scattering from acoustic phonons and inelastic scattering from LO phonons for $n_s=1\times 10^{11}$ cm^{-2}: (a) $T=20$ K; (b) enlargement of the low-energy part; (c) $T=300$ K. The thin solid line is the total relaxation rate due to acoustic phonons $\tau_{\rm ac}^{-1}$. $D=12$ eV and $n_{\rm depl}=5\times 10^{10}$ cm^{-2}.

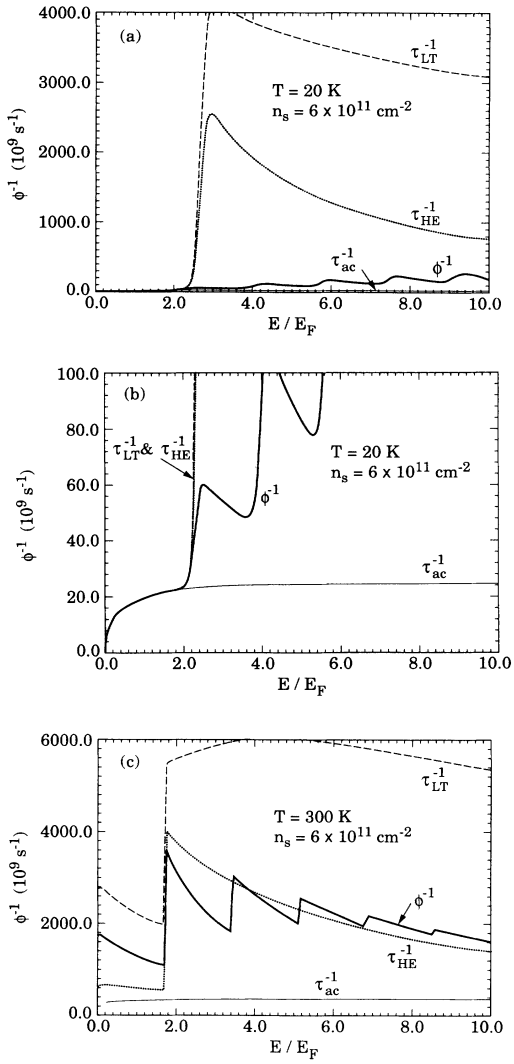

FIG. 15. The perturbation function $\phi^{-1}(E)$ (thick solid line), low-temperature relaxation rate $\tau_{\rm LT}^{-1}$ (dashed line), and high-energy relaxation rate $\tau_{\rm HE}^{-1}$ (dotted line) due to quasielastic scattering from acoustic phonons and inelastic scattering from LO phonons for $n_s=6\times 10^{11}$ cm^{-2}: (a) $T=20$ K; (b) enlargement of the low-energy part; (c) $T=300$ K. The thin solid line is the total relaxation rate due to acoustic phonons $\tau_{\rm ac}^{-1}$. $D=12$ eV and $n_{\rm depl}=5\times 10^{10}$ cm^{-2}.

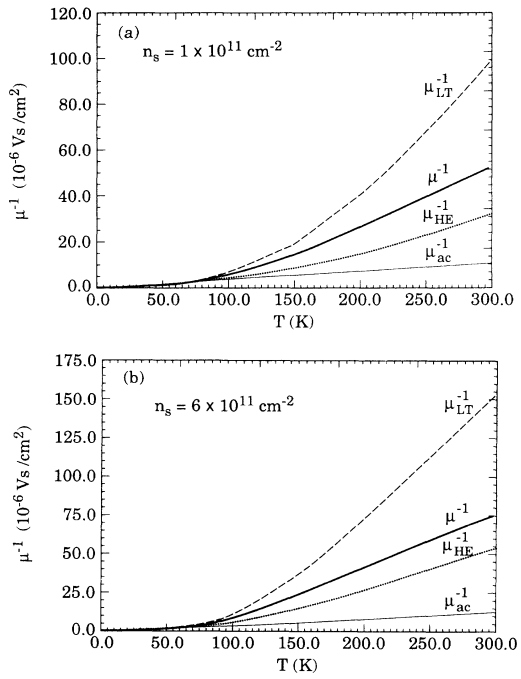

FIG. 16. The reciprocal mobility limited by acoustic and polar LO phonons (thick solid line) and approximations based on the low-temperature relaxation rate τ_{LT}^{-1} (dashed line) and the high-energy relaxation rate τ_{HE}^{-1}: (a) $n_s = 1 \times 10^{11}$ cm^{-2}; (b) $n_s = 6 \times 10^{11}$ cm^{-2}. The thin solid line is the reciprocal acoustic-phonon limited mobility μ_{ac}^{-1}. The depletion density $n_{depl} = 5 \times 10^{10}$ cm^{-2} and $D = 12$ eV.

approximations are given in Fig. 16(a) and 16(b). We see that at room temperature the low-temperature relaxation rate τ_{LT}^{-1} underestimates the true mobility by about a factor of 2. The high-energy relaxation rate overestimates the true mobility τ_{HE}^{-1} but the deviation from the iterative value is much less.

IV. CONCLUSIONS

In summary, we have presented a detailed investigation of the phonon-scattering rate and phonon-scattering-limited mobilities in an $Al_xGa_{1-x}As/GaAs$ heterojunction in the temperature range $T = 1-300$ K. We considered the quasielastic scattering from the DP and PE-coupled acoustic phonons, and the inelastic scattering from the polar LO phonons. Our calculations were based on the following model and approximations: (1) the electrons were assumed to occupy only the lowest subband; (2) the subband wave function in the z direction was approximated by the standard variational wave function; (3) we assumed the bulk phonons to be the only phonons contributing to scattering; and (4) the DP and PE-coupled acoustic-phonon-scattering rates were calculated with full wave vector and temperature-dependent static screening of the electron-phonon interaction included in the RPA.

In the EP regime we carried out a detailed investigation of the linear coefficient of the temperature dependence of the low-temperature mobility α. In excellent agreement with experimental results we showed that the curious minima in $\alpha(n_s)$ can be explained with an enhanced value of the DP constant, without a corresponding arbitrary enhancement of the PE constant, by taking into account the temperature-dependent effects of screening and thermal broadening at low carrier densities. In the BG regime we computed the relaxation rates and explicitly showed the drastic reduction that occurs at the Fermi energy at low enough temperatures. As a result, the calculated reciprocal mobilities exhibited a stronger dependence (the effective exponent increasing from 1 in the EP regime to about 4.5 in the BG regime) on the temperature T than the corresponding EP mobilities. For high temperatures the perturbation distribution was calculated by solving the linearized Boltzmann equation via the Ritz iteration method of Rode. The direct solution was compared with the closed expressions of the approximate relaxation times at low temperatures τ_{LT} and high energies τ_{HE} to check their level of validity.

The calculations presented can be extended and improved upon in a number of ways. A quantitatively more accurate model can be constructed by using numerical subband wave functions,[47] and including the effects of intersubband scattering[48] which certainly become important at room temperatures and high carrier densities. The possible contribution of interface phonons to electron scattering, and the effects of dynamical screening[49] of the LO phonons, can also be considered.

It has been found that for the total average energy-loss rate of a 2DEG in a $Al_xGa_{1-x}As/GaAs$ heterojunction at low temperatures, the inclusion of the renormalized LO-phonon contribution to the standard acoustic-phonon theory with the *bulk* value for D is in close agreement with the experimental data for high densities. If these low-energy modes of the renormalized LO phonons are important in the context of energy relaxation, it is then natural to speculate whether they also contribute significantly to the momentum relaxation of the electron. It is possible that such an analysis (which must incorporate complicated vertex corrections) may reconcile the DP constant value in the corresponding transport problem.

Our calculated results for the temperature and density dependence of the phonon-scattering-limited electronic mobility are in excellent quantitative agreement with the available experimental results,[43,44] establishing the basic validity of the model. The value of the DP coupling constant needed for this excellent agreement between theory and experiment is around 12 eV, which is consistent with earlier theoretical claims.[27,37] Real systems obviously always contain impurities which contribute to scattering as well. In ultrahigh-mobility samples one can rather accurately extract the phonon scattering contribution to the electronic mobility by extrapolating the inverse mobility μ^{-1} to zero temperature and subtracting out the zero-temperature contribution μ_0^{-1}, assuming that $\mu^{-1} = \mu_0^{-1} + \mu_{ph}^{-1}(T)$ with our calculated results of this paper applicable to the phonon part μ_{ph}^{-1}. For lower mobili-

ty samples ($\mu < 10^5$ cm^2/V s), impurity scattering starts[26] contributing significantly to the temperature dependence of mobility and this separation (or the zero-temperature extrapolation) fails to give the correct phonon-scattering-limited mobility. We expect our theoretical results to be widely applicable to high-mobility heterojunctions.

ACKNOWLEDGMENTS

This work was supported by the U.S. Army Research Office (ARO), the U.S. Office of Naval Research (ONR), the National Center for Supercomputing Applications (NCSA) at the University of Illinois at Urbana-Champaign.

[1]J. H. English, A. C. Gossard, H. L. Störmer, and K. W. Baldwin, Appl. Phys. Lett. **50**, 1826 (1987).
[2]L. Pfeiffer, K. W. West, H. L. Störmer, and K. W. Baldwin, Appl. Phys. Lett. **55**, 1888 (1989).
[3]B. R. Nag, in *Electron Transport in Compound Semiconductors,* edited by M. Cardona, P. Fulde, and H.-J. Queissier, Springer Series in Solid-State Sciences Vol. 11 (Springer, New York, 1980).
[4]P. K. Basu and B. R. Nag, Phys. Rev. B **22**, 4849 (1980).
[5]P. J. Price, Surf. Sci. **143**, 145 (1984).
[6]P. J. Price, Ann. Phys. (N.Y.) **133**, 217 (1981).
[7]P. J. Price, Surf. Sci. **113**, 199 (1982).
[8]B. K. Ridely, J. Phys. C **15**, 5899 (1982).
[9]P. J. Price, J. Vac. Sci. Technol. **19**, 599 (1981).
[10]P. F. Maldague, Surf. Sci. **73**, 296 (1978).
[11]S. Das Sarma, Phys. Rev. B **33**, 5401 (1986).
[12]S. Das Sarma and F. Stern, Phys. Rev. B **32**, 8442 (1985).
[13]G. D. Mahan, *Many Particle Physics* (Plenum, New York, 1981).
[14]T. Holstein, Ann. Phys. (N.Y.) **29**, 410 (1964).
[15]P. J. Price, Solid State Commun. **51**, 607 (1984).
[16]H. L. Störmer, L. N. Pfeiffer, K. W. Baldwin, and K. W. West, Phys. Rev. B **41**, 1278 (1990).
[17]D. J. Howarth and E. H. Sondheimer, Proc. R. Soc. London, Ser. A **219**, 53 (1953); B. F. Lewis and E. H. Sondheimer, *ibid.* **227**, 241 (1955); N. N. Grigor'ev, I. M. Dykman, and P. M. Tomchuk, Fiz. Tverd. Tela (Leningrad) **10**, 1058 (1968) [Sov. Phys. Solid State **10**, 837 (1968)]; R. T. Delves, Proc. Phys. Soc. **73**, 572 (1959); K. Fletcher and P. N. Butcher, J. Phys. C **5**, 212 (1972); H. D. Rees, J. Phys. Chem. Solids **30**, 643 (1969); A. Fortini, D. Diguet and J. Lugand, J. Appl. Phys. **41**, 3121 (1970); W. Fawcett, A. D. Boardmann, and H. D. Rees, Solid State Commun. **6**, 305 (1968).
[18]B. Vinter, Appl. Phys. Lett. **45**, 581 (1984).
[19]B. Vinter, Surf. Sci. **170**, 445 (1986).
[20]D. L. Rode, Phys. Rev. B **2**, 1012 (1970).
[21]D. L. Rode, in *Semiconductors and Semimetals,* edited by R. K. Willardson and A. C. Beer (Academic, New York, 1975), Vol. 10, pp. 1–89.
[22]B. R. Nag, J. Phys. C **7**, 3541 (1974).
[23]H. Fröhlich, Adv. Phys. **3**, 325 (1974).
[24]H. Fröhlich, Proc. R. Soc. London, Ser. A **171**, 496 (1937).
[25]T. Ando, J. Phys. Soc. Jpn. **51**, 3900 (1982).
[26]F. Stern and S. Das Sarma, Solid State Electron. **28**, 211 (1985).
[27]E. E. Mendez, P. J. Price, and M. Heiblum, Appl. Phys. Lett. **45**, 294 (1984).
[28]K. Hirakawa and H. Sakaki, Phys. Rev. B **33**, 8291 (1986).
[29]B. J. F. Lin, D. C. Tsui, and G. Weimann, Solid State Commun. **56**, 287 (1985).
[30]M. A. Paalanen, D. C. Tsui, A. C. Gossard, and J. C. M. Hwang, Phys. Rev. B **29**, 6003 (1984).
[31]C. M. Wolfe, G. E. Stillman, and W. T. Lindley, J. Appl. Phys. **41**, 3088 (1970).
[32]W. Walukiewicz, H. E. Ruda, J. Lagowski, and H. C. Gatos, Phys. Rev. B **30**, 4571 (1984).
[33]Y. Okuyama and N. Tokuda, Phys. Rev. B **40**, 9744 (1989).
[34]K. Lee, M. S. Shur, T. J. Drummond, and H. Morkoç, J. Appl. Phys. **54**, 6432 (1983).
[35]P. J. Price, Phys. Rev. B **32**, 2643 (1985).
[36]W. Walukiewicz, H. E. Ruda, J. Lagowski, and H. C. Gatos, Phys. Rev. B **32**, 2645 (1985).
[37]B. Vinter, Phys. Rev. B **33**, 5904 (1986).
[38]S. J. Manion, M. Artaki, M. A. Emanuel, J. J. Coleman, and K. Hess, Phys. Rev. B **35**, 9203 (1987).
[39]K. Hirakawa and H. Sakaki, Appl. Phys. Lett. **49**, 889 (1986).
[40]P. J. Price, J. Appl. Phys. **53**, 6863 (1982).
[41]J. K. Jain, R. Jalabert, and S. Das Sarma, Phys. Rev. Lett. **60**, 353 (1988); S. Das Sarma, J. K. Jain, and R. Jalabert, Phys. Rev. B **41**, 3561 (1990).
[42]T. Kawamura, S. Das Sarma, R. Jalabert, and J. K. Jain, Phys. Rev. B **42**, 5407 (1990).
[43]J. J. Harris, C. T. Foxon, D. Hilton, J. Hewett, C. Roberts, and S. Auzoux, Surf. Sci. **229**, 113 (1990).
[44]T. Kawamura and S. Das Sarma, Phys. Rev. B **42**, 3725 (1990).
[45]T. Ando, A. B. Folwer, and F. Stern, Rev. Mod. Phys. **54**, 499 (1982).
[46]F. Stern, Phys. Rev. Lett. **44**, 1469 (1980).
[47]F. Stern and S. Das Sarma, Phys. Rev. B **30**, 840 (1984).
[48]E. D. Siggia and P. C. Kwok, Phys. Rev. B **4**, 1024 (1970); F. Stern, Surf. Sci. **73**, 197 (1978); S. Mori and T. Ando, Phys. Rev. B **19**, 6433 (1979).
[49]X. L. Lei, J. Phys. C **18**, L593 (1985).